Individual Thresholding of Voxel-based Functional Connectivity Maps

Estimation of Random Errors by Means of Surrogate Time Series

L. Griffanti[1,2]; F. Baglio[1]; M. M. Laganà[1]; M. G. Preti[1,2]; P. Cecconi[1]; M. Clerici[1,3]; R. Nemni[1,3]; G. Baselli[2]

[1]MR Laboratory, IRCCS Fondazione Don Carlo Gnocchi, Milan, Italy;
[2]Department of Electronics, Information and Bioengineering, Politecnico di Milano, Milan, Italy;
[3]Università degli Studi di Milano, Milan, Italy

Keywords

Magnetic resonance imaging, functional connectivity, resting state, surrogate time series

Summary

Introduction: This article is part of the Focus Theme of *Methods of Information in Medicine* on "Biosignal Interpretation: Advanced Methods for Neural Signals and Images".

Background: Voxel-based functional connectivity analysis is a common method for resting state fMRI data. However, correlations between the seed and other brain voxels are corrupted by random estimate errors yielding false connections within the functional connectivity map (FCmap). These errors must be taken into account for a correct interpretation of single-subject results.

Objectives: We estimated the statistical range of random errors and propose two methods for an individual setting of correlation threshold for FCmaps.

Methods: We assessed the amount of random errors by means of surrogate time series and described its distribution within the brain. On the basis of these results, the FCmaps of the posterior cingulate cortex (PCC) from 15 healthy subjects were thresholded with two innovative methods: the first one consisted in the computation of a unique (global) threshold value to be applied to all brain voxels, while the second method is to set a different (local) threshold of each voxel of the FCmap.

Results: The distribution of random errors within the brain was observed to be homogeneous and, after thresholding with both methods, the default mode network areas were well identifiable. The two methods yielded similar results, however the application of a global threshold to all brain voxels requires a reduced computational load. The inter-subject variability of the global threshold was observed to be very low and not correlated with age. Global threshold values are also almost independent from the number of surrogates used for their computation, so the analyses can be optimized using a reduced number of surrogate time series.

Conclusions: We demonstrated the efficacy of FCmaps thresholding based on random error estimation. This method can be used for a reliable single-subject analysis and could also be applied in clinical setting, to compute individual measures of disease progression or quantitative response to pharmacological or rehabilitation treatments.

Correspondence to:
Ludovica Griffanti
MR Laboratory, Fondazione Don Carlo Gnocchi ONLUS, IRCCS S. Maria Nascente
via Capecelatro 66
20148 Milan
Italy
E-mail: lgriffanti@dongnocchi.it

Methods Inf Med 2015; 54: 227–231
http://dx.doi.org/10.3414/ME13-02-0042
received: October 21, 2013
accepted: January 24, 2014
prepublished: May 9, 2014

1. Introduction

Voxel-based functional connectivity (FC) analysis (also called seed-based FC) was the first technique used for the analysis of resting state fMRI data [1] and it is still extensively applied [2, 3]. The simplicity of the method, its straightforward interpreta-bility with respect to the other methods, and its moderate to high reliability [4], make voxel-based FC an attractive and use-ful approach.

The functional connectivity map (FCmap) is usually computed as Pearson's linear correlation between the signal extracted from a specific region of interest (seed) and all the other brain voxels, show-ing the network of regions functionally connected with the seed [5]. In a recent study, Hlinka and colleagues [6] demon-strated that, after standard fMRI prepro-cessing steps, linear correlation well cap-tures the full functional connectivity. Addi-tionally, spatial and temporal filtering further diminish small nonlinearities in the data. However, some linear correlations could be artefactual, i.e. due to chance and not to real FC, and the p-value associated to Pearson's correlation coefficient, al-though significant *per se*, is not indepen-dent from this random error.

To our knowledge, these random errors are usually ignored and significant con-nected voxels are detected only at group level. At single-subject level, the use of an arbitrary threshold without the quantifi-cation of the random error size could lead to misinterpretation of the FC map, bias the extraction of quantitative information, and affect the final results when used in

combination with other imaging modalities, (e.g. in neurosurgical planning) [7].

For this reason, in voxel-based FC analyses, a more reliable method is needed for the identification of voxels significantly connected with the seed, taking into account for random errors.

In this work we describe a method for the estimation of this random error by using surrogate time series. Moreover, two thresholding methods are proposed for a reliable analysis of single-subject FC maps.

2. Methods

Resting state fMRI data were acquired from 15 healthy subjects (age: 46.6 ± 23.0 years; six males) with a 1.5T Siemens scanner. Each volunteer underwent a 3D high resolution T1-weighted sequence (TR/TE = 1900/3.37 ms; voxel size = 1 × 1 × 1 mm^3) and a 7 min 30 sec EPI run with BOLD contrast (TR/TE = 2500/30 ms; voxel size = 3 × 3 × 2.5 mm^3; 180 volumes) in resting state condition (they were instructed to be relaxed, with eyes closed, not to think anything in particular and not to fall asleep). All subjects provided written informed consent to participate in the study according to the recommendations of the declaration of Helsinki.

The starting preprocessing steps, performed with SPM8, involved the following: 1) correction for slice-timing differences; 2) correction of head motion across functional images; 3) coregistration to the anatomical image and spatial normalization to the MNI space with a voxel size of 3 × 3 × 3 mm^3; 4) spatial smoothing with a 4 mm full-with at half-maximum Gaussian kernel. Then, further steps specific for resting state fMRI were: 5) regression of nuisance variables (head motion, mean white matter signal and mean cerebrospinal fluid signal); 6) temporal pass-band filtering (0.01– 0.08 Hz) to remove linear trends and constant offsets over each run. For these operations we used REST toolbox [8].

For each subject, a region of interest (ROI) of 6 mm radius was positioned in the posterior cingulate cortex (with center at MNI coordinates: 0 –53 26) based on previous studies [9, 10]. This area plays a central role in the default mode network (DMN), the principal and more investigated resting state network. The corresponding time series (PCC-time course) was extracted as the mean signal within the ROI. Voxel-based functional connectivity map (FCmap) was then obtained by computing the linear correlation between the PCC-time course and the time courses of all acquired voxels. Correlation maps were then converted to z-maps using Fisher's r-to-z transformation (zFCmap).

Surrogate time series of the PCC-time course were constructed with the iteratively refined amplitude adjusted Fourier transform (iAAFT) method, proposed by Schreiber and Schmitz [11]. First, the Fourier transform of the series was computed to impose the amplitude spectrum (second order properties). A white series with random phases was then created by shuffling the original series. Reordering the series, a random phase surrogate with original probability distribution was provided. Deviations in spectrum and distribution from the goal set were iteratively corrected. In this way, the obtained iAAFT surrogates preserved both amplitude distribution and spectral shape of the original time series, but the phases were randomized.

From the PCC-time course of each subject, 39 surrogate series were generated. Voxel-based functional connectivity was then computed using each surrogate time series as seed. Since the temporal information of the PCC-time course has been destroyed in the surrogates, no more correlation is expected between brain voxels and the seed. Any correlation in the new FCmap is due to chance, so we obtained a set of 39 random error maps and the corresponding z-maps (zERR).

For each brain voxel, the mean and the standard deviation of the random error among the 39 maps was computed. Thus, we obtained an error mean map (meanERRmap) and an error standard deviation map (stdERRmap) for each subject, whose distributions were fitted to theoretical sample distributions, respectively the normal distribution and the chi-square distribution, using maximum likelihood estimation method on shape parameters.

The mean values of meanERRmap and stdERRmap distributions (respectively $\overline{m}$ and $\overline{std}$) were then used to compute a 2 * std (i.e., $p < 0.05$) confidence interval (CI) with Equation 1:

$$CI_{global} = \overline{m} \pm 2 * \overline{std} \quad (1)$$

The boundaries of this CI (Tsup and Tinf) were then used as threshold values and applied to all voxels of zFCmaps (global thresholding): only voxels showing a correlation value higher than Tsup or lower than Tinf were considered as significantly connected with the seed.

A possible alternative to this thresholding method was to apply a different threshold to each voxel, according to the amount of random error.

For this local thresholding, the 2 * std ($p < 0.05$) CI was computed for each brain voxel (i) using ▶Equation 2:

$$CI_{local}(i) = mean(zErr(i)) \pm 2 * std(zERR(i)) \quad (2)$$

In this way, two additional maps were generated for each subject: the superior confidence interval map (supCImap) and the inferior confidence interval map (infCImap). Finally, zFCmaps were thresholded using supCImap and infCImap: voxels showing a correlation value out of the CI were considered as significantly connected with the seed.

The thresholded maps obtained with the two methods were compared by calculating the Dice's index as similarity measure, and evaluating the difference in the number of voxels that passed the thresholds (paired t-test).

For global thresholding, mean and standard deviation of T_{sup} and T_{inf} across subjects were computed and their correlation with age was tested in order to evaluate the inter-subject variability of CI_{global}. Finally, the variability due to the number (N) of surrogates used, was assessed repeating the computation of random error and CI_{global} values with N = 2 : 39.

3. Results

In Figure 1, the meanERRmap and stdERRmap of one subject are shown as examples, as well as their distributions. The mean and standard deviation values of ran-

dom error are spatially homogeneous within the brain and the relative distributions were found to be well fitted by corresponding theoretical distributions.

The PCC-zFCmap of one subject before (a) and after global (b) and local (c) random error thresholding is illustrated in ▶Figure 2. With both methods, the principal DMN areas (posterior cingulate cortex, medial prefrontal cortex and inferior parietal lobule) are well identifiable. Comparing the two thresholded maps, the mean Dice's index across subjects was 0.81 ± 0.04 and the number of voxels significantly connected with the seed obtained using global and local thresholding was not significantly different (N voxel after global thresholding = 9144.400 ± 3522.104; N voxel after local thresholding = 9322.330 ± 3755.627; p = 0.429, paired t-test).

Regarding inter-subjects variability of global threshold, CI_{global} standard deviation across subjects was very low compared to its mean value (Tsup(z) = 0.252 ± 0.008,

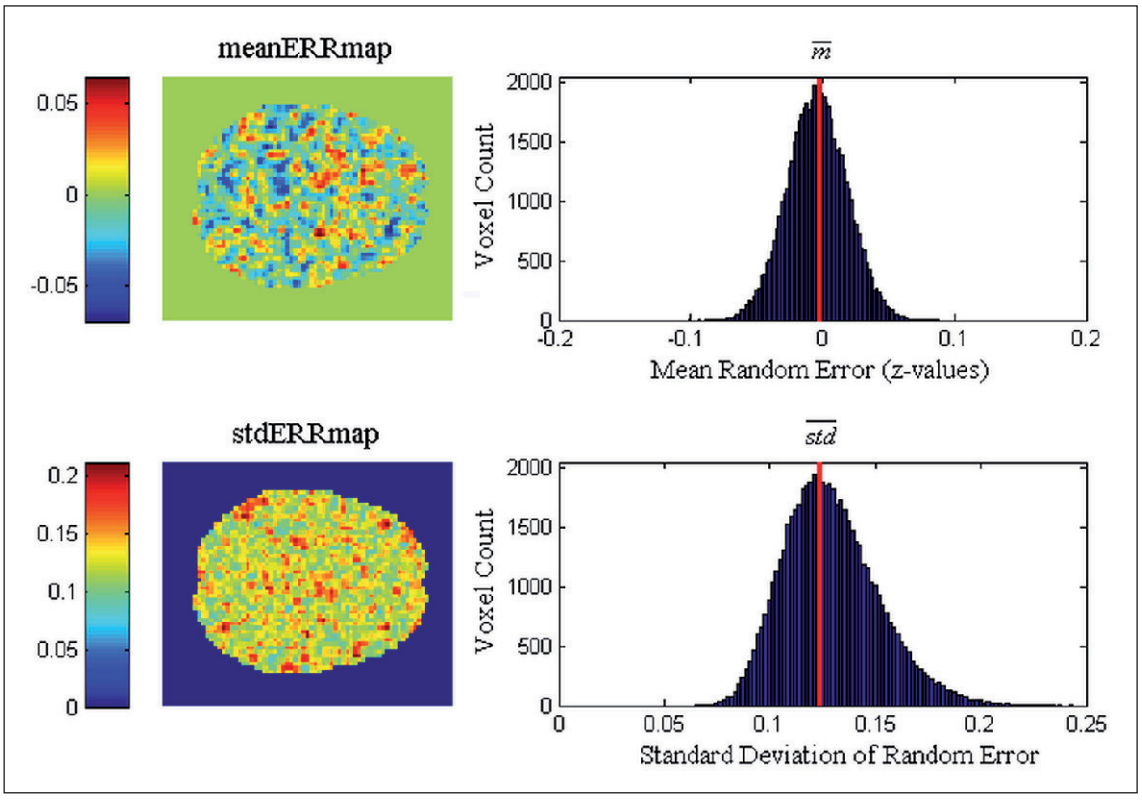

Figure 1
Random Error estimation. The mean random error (top panel) is spatially homogeneous within the brain and the distribution is Gaussian-shaped centered in zero. Also the standard deviation of the random error (bottom panel) is homogeneous with chi-square distribution. Data relative to a 20-year female healthy subject.

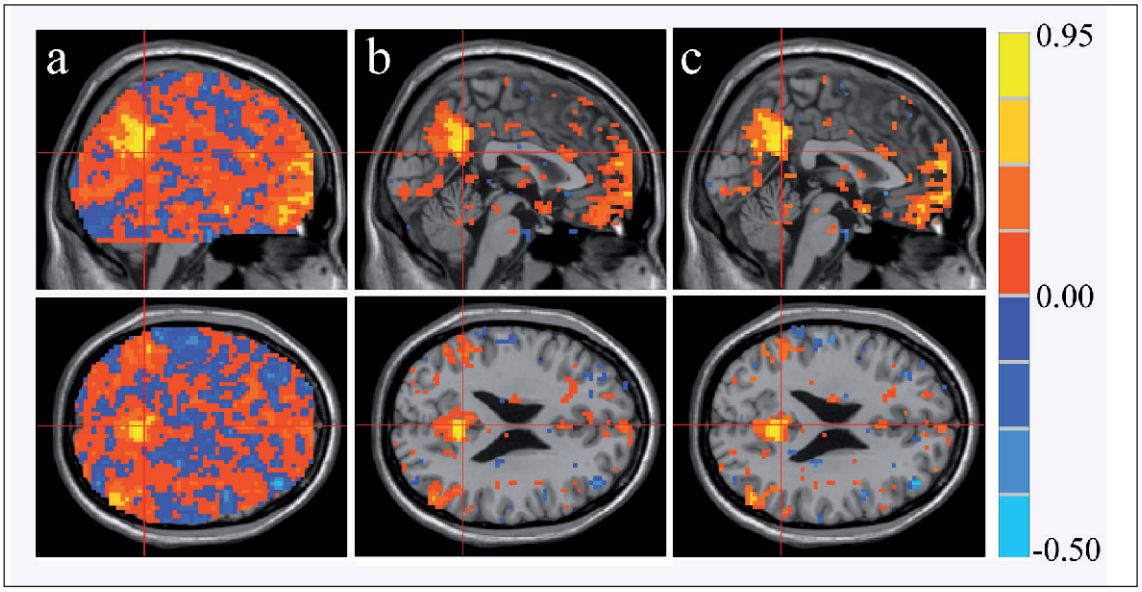

Figure 2
Random error thresholding. The single-subject PCC-FCmap is shown before (a) and after global (b) and local (c) random error thresholding. It can be observed that, after thresholding, DMN areas are well identifiable.

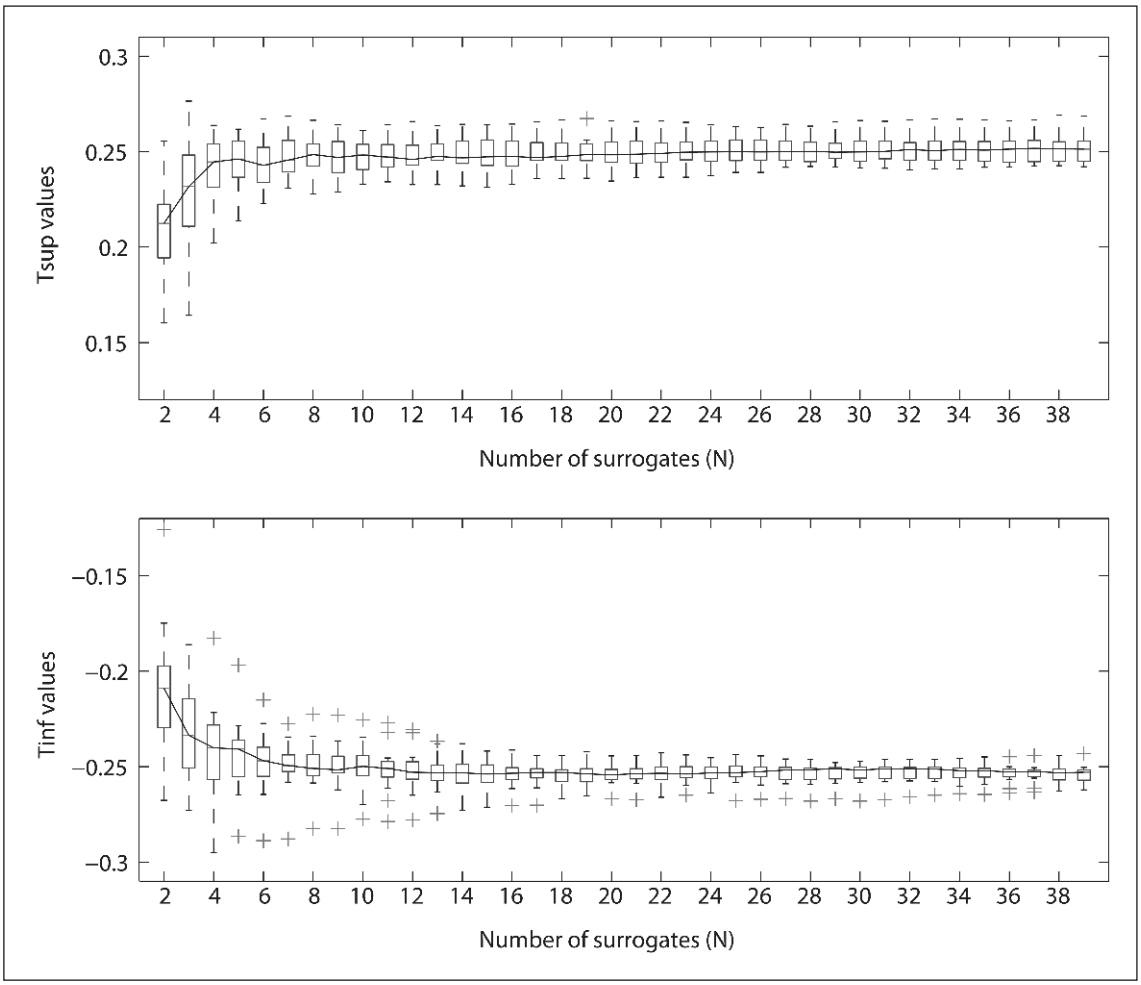

Figure 3
Global confidence interval (CI_{global}) variability. The boxplots illustrate the distribution across subjects of the upper boundary (Tsup, top panel) and lower boundary (Tinf, bottom panel) of CI_{global}, for different number of surrogates used for their computation.

Tinf(z) = −0.254 ± 0.005) and not correlated with age (correlation Tsup-age: p = 0.28; correlation Tinf-age: p = 0.34). Obtaining a mean global threshold of z = ± 0.25 (corresponding to a correlation coefficient r = 0.245), the associated p-value for a Pearson probability distribution is $p < 0.001$. As shown in Figure 3, this small variability is quite independent from the number of surrogates and CI_{global} boundaries reach stable values using a small number of surrogates ($N \approx 10$).

4. Discussion and Conclusions

In this work we examined the problem of random errors in voxel-based functional connectivity analyses and proposed a method for error evaluation based on surrogate time series. Observing a homogeneous distribution of random error within the brain, we can infer that there are no regions more influenced by random error than others and that this kind of error is independent from the resting state activity.

Random errors are usually ignored in this kind of analysis and correction is only performed at group level. In order to perform a reliable single-subject analysis, we proposed two individual thresholding methods, which allow the identification of voxels significantly connected with the seed region. The two methods have been proven to be effective in identifying the DMN areas and are substantially equivalent, although the global thresholding approach requires a reduced computational load and may be preferable for further analyses. The boundary values of the CI_{global} have a low inter-subject variability not depending from subjects' age. Moreover the number of surrogates needed for the analysis can be reduced, further decreasing the computational load required for the analyses without significant changes in the results.

The proposed method is promising for an application in a clinical setting to extract quantitative information about FC alterations with respect to a seed ROI and to be used as part of multimodal imaging tools [7]. Indeed, the availability of a reliable single-subject FC analysis could be particularly useful for rare case studies (when a group study is not feasible), for neurosurgical planning, and for the longitudinal evaluation of a single patient's disease progression or response to pharmacological treatments or rehabilitation.

References

1. Biswal B, Yetkin FZ, Haughton VM, Hyde JS. Functional connectivity in the motor cortex of resting human brain using echo-planar MRI. Magn Reson Med 1995; 34 (4): 537–541.

2. Cole DM, Smith SM, Beckmann CF. Advances and pitfalls in the analysis and interpretation of resting-state FMRI data. Front Syst Neurosci 2010; 4: 8.
3. Fox MD, Greicius M. Clinical applications of resting state functional connectivity. Front Syst Neurosci 2010; 4: 19.
4. Shehzad Z, Kelly AM, Reiss PT, Gee DG, Gotimer K, Uddin LQ, et al. The resting brain: unconstrained yet reliable. Cereb Cortex 2009; 19 (10): 2209 –2229.
5. Fox MD, Raichle ME. Spontaneous fluctuations in brain activity observed with functional magnetic resonance imaging. Nat Rev Neurosci 2007; 8 (9): 700 –711.
6. Hlinka J, Palus M, Vejmelka M, Mantini D, Corbetta M. Functional connectivity in resting-state fMRI: is linear correlation sufficient? Neuroimage 2011; 54 (3): 2218 –2225.
7. Berks G, Pohl G, Keyserlingk DG. 3D-VIEWER: an atlas-based system for individual and statistical investigations of the human brain. Methods Inf Med 2001; 40 (3): 170 –177.
8. Song XW, Dong ZY, Long XY, Li SF, Zuo XN, Zhu CZ, et al. REST: a toolkit for resting-state functional magnetic resonance imaging data processing. PLoS One 2011; 6 (9): e25031.
9. Van Dijk KR, Hedden T, Venkataraman A, Evans KC, Lazar SW, Buckner RL. Intrinsic functional connectivity as a tool for human connectomics: theory, properties, and optimization. J Neurophysiol 2010; 103 (1): 297– 321.
10. Andrews-Hanna JR, Snyder AZ, Vincent JL, Lustig C, Head D, Raichle ME, et al. Disruption of large-scale brain systems in advanced aging. Neuron 2007; 56 (5): 924 – 935.
11. Schreiber T, Schmitz A. Surrogate time series. Physica D 2000; 142 (3–4): 346 –382.